AIAA 95-2826

3-D Monte-Carlo Particle-in-Cell Simulations of Ion Thruster Plasma Interactions

J. Wang and J. Brophy
Jet Propulsion Laboratory
California Institute of Technology
Pasadena, CA 91109

31st AIAA/ASME/SAE/ASEE
Joint Propulsion Conference and Exhibit
July 10-12, 1995 / San Diego, CA

3-D Monte-Carlo l'article-i~l-Cdl Simulations of Ion Thruster Plasma Interactions

California Institute of Technology, Pasadena

1. Introduction

Electric propulsion devices arc valued as a high-specific impulse class of space propulsion system. Currently, there is substantial interest in the use crf ion propulsion for enhancing the capabilities of Discovery Class spacecraft. The usc of xenon ion propulsion will also enable many planned Ncw Millennium missions to be performed within the time aud cost constraints. To baseline the usc of ion propulsion on spacecraft, NASA has initiated a technology demonstration and validation program NSTAR (NASA SEP Technology Application Readiness). Through ground tests and space flight experiments, NSTAR will validate the life arid performance of xenon ion thrusters, characterize the benefits arid tradeoffs of using xenon ion thrusters, and study the interactions and any potential impacts induced by ion thrusters.

Due to their intrinsic complex nature, our current understanding of certain aspects of ion thruster interactions is still limited. Mauy important issues, including iou thruster plumes and ion acceleration processes, arc still subjects of active research. Cost and complexity of space experiments preclude the possibility of performing the parametric studies needed to study all possible interaction scenarios, while boundary effects and the difficulty of matching space conditions in a laboratory make it difficult to extrapolate laboratory results directly to the space environment. Hence, rigorous theoretical models based on fundamental physics laws arc needed to complement the NSTAR and other exper - ments. Currently we are undertaking a modeling study iu support of the NSTAR program and other ad vanced propulsion research activities at JPL. This paper discusses our work of modeling ion thruster plumes and interact ions.

In section 2 of this paper, we first provide a brief overview and then discuss our formulation and approach. The numerical models wc are developing arc based on three-dimensional (3-D) electrostatic and electromagnetic Particle-in-Cell Monte Carlo collision (PIC-MCC) simulations. In section 3, we present simulation results for single and multiple thruster plumes. We also discuss charge exchange ion backflows under ground Lest and in space conditions. Section 4 contains a summary and conclusions.

2. Simulation Models and Algorithms

In ion thrusters, propellant ions arc accelerated electrostatically to form a high velocity beam along with neutralizing electrons. An ion thruster plume is composed of propellant efflux (beam ions, neutralizing electrons, and unionized neutrals escaped through the iou optics and from the neutralizer), nonpropellant e fflux (material sputtered fi orn thruster components and the neutralizer), and a low-energy charge-exchange plasma (generated through collisions between energetic ions and the neutrals within the plume). The plasma plume has raised var ious concerns. For instance, the charge-exchange ions can leave the primary plume and backflow toward the spacecraft. Backflow charge-exchange ious arc thought to be the major mechanism for accelerator grid erosion. The deposition of the plume particles ou thermal and optical surfaces may result in change of the surface properties. The plume represents additional charging mechanisms, which may induce plasma interactions with solar arrays. The high energy ion beam may also generate plasma waves and instabilitics through twain plasma interactions, and thus induce electromagnetic interfer ence. The effects of plasma plume on ambient charged particles may contaminate

*Member Technical Staff, Advanced Propulsion, Member AIAA
†Supervisor, Advanced Propulsion, Member AIAA

the results of certain in situ measurements. Although the xenon ion engine has a substantially lower contamination potential compared to other types of thrusters, nevertheless, the interactions induced must be fully understood and their impacts quantified.

Ion thruster plasma interactions nave been studied for some time. However, duc to the complexity of the problem, theoretical models developed in most previous studies [1 1, 2, 1] arc mainly empirically based analytical models with ad hoc approximations and oversimplifications involved in their formulations. Computer particle simulation offers an approach to establish first-principle based models. A particle simulation code models a plasma as many test particles and follows the evolution of the orbits of individual test particles in the self-consistxmtly computed macroscopic force field. In principal, such an approach is limited only by t he computing power.

Recently, two sets of studies have used the particle simulation method to address issues realted to ion thrusters. Peng et al used electrostatic PIC-MCC simulations to model the immediate downstream region of thruster accelerator grids and study grid erosion problems[7, 8, 9]. Samanta Roy et, al used electrostatic PIC simulations to model the far-downstream region and study charge exchange ion backflow[12, 4, 13]. In the model developed by Samanta Roy et al, the primary ion beam is modeled by a given steady density profile $n_{bi}(r, z)$ and charge-exchange ions arc treated as test particles, which are generated in the simulation domain using a volumetric production rate calculated from the ion beam density and neutral density profile:

$$dN_{cex}(x)/dt = n_n(x) n_{bi}(x) v_{bi} \sigma_{cex}(v_{bi})$$

In both the Peng et al and the Samanta Roy et al studies, electrons are modeled as a Boltzmann distribution

$$n_e = n_0 \exp(e(\Phi - Phi_0)/KT_e) \qquad (1)$$

where n_0 and Φ_0 arc the electron density and potential at a reference point respectively (Samanta Roy et al further modified the Boltzman distribution with a variable electron temperature), and the Poisson's equation is solved. While an electrostatic hybrid PIC approach is very effective in studying the physics related to the ions, it cannot bc applied to study situations where the electron dynamics plays au important role, such as the "intermediate" downstream region and the near-field of a plasma bridge neutralizer, or electromagnetic interactions. Treating the primary ion beam analytically also makes the model difficult to apply to multiple thruster plumes where interactions between two ion beams may be important.

In this study, we move towards a more generalized model. Figure 1 illustrates the simulation models being developed and algorithms used. The simulation models include one for ground tests and one for ill-space conditions. Depending on the nature of the problem, either 3-1) hybrid electrostatic (ES) PIC-MCC simulation, or full particle ES PIC-MCC simulation, or full particle electromagnetic (EM) PIC-MCC simulation can be performed.

Tile hybrid code is similar to that of Peng et al and Samanta et al where it is assumed that the electron density n_e is given by the Boltzmann distribution eq(1). In the two full particle codes, rather than modeling the beam ions with an analytical density profile and electrons wit h a variable temperature Boltzman distribution, wc model ail species of charged particles (i.e. primary beam ions, neutralizing electrons, collision-generated ions and electrons) as test particles. In all three codes, rather than using a volumetric charge-cxcliallgc ion production model, wc perform Monte Carlo collision calculation for all test particles. Various initial and boundary conditions may be incorporated into the model depending on the problem setup. Figure 2 shows typical simulation setups used in the full particle code for single thruster aud multiple thrusters. Currently, the code is set to simulate the region down stream of the thruster exit, which is in the x direction.

The neutrals are treated as a steady state background. As in [4], the density distribution of the neutral plume is modeled as that of a free molecular flow from a point source located at one thruster radius r_T behind the thruster exit

$$n_{np}(R, \theta) = a n_{n0} (1 - (1 - 1 (\frac{r_T}{R})^2)^{-1/2}) \cos\theta \qquad (2)$$

where R is the distance to the point source, θ is the angle between R and the x axis, anti a is a correction factor. To simulate ground test situations, a constant neutral density n_{ng} determined by the test chamber pump may be added to the background.

At eat]] time step, the propellant ions are injected into t he simulation domain from the thruster exit. To simulate the iou beam current emitted from the thruster, the particles are injected in such a way that the resulting flux has a density in Gaussian distribution at the exit plan

$$|J_{bi}| = J_{bi0} \exp(- (r/r_T)^2), \; r \le r_T \qquad (3)$$

where J_{bi0} is the density al the thrsuter center and r is the distance to the center on the thruster exit plan, and a divergence angle similar to that of measured in experiments. (The divergence angle is observed to be about 25").

In full particle simulations, electrons are also injected into the simulation domain from the neutralizer. The injected electrons are assumed to follow a Maxwellian distribution. (The thermal energy of the emitted electrons is observed to be of 1 --5 eV.).

As in a standard PIC-MCC code[?], the trajectory of each particle is integrated from

$$\frac{dm\vec{V}}{dt} = \vec{F} = q(\vec{E} + \vec{V} \times \frac{\vec{B}}{c}), \quad \frac{d\vec{x}}{dt} = \vec{V} \qquad (4)$$

using a standard leapfrog scheme. The probability that a charged particle suffers a collision within time t is given by

$$P(t) = 1 - \exp(-\int_0^t \nu(t)dt) \qquad (5)$$

where v = $n_n(\vec{x})v\sigma(v)$ is the total collision frequency. Since the neutral density, which is defined on grid points, is nonuniform, the collision frequency for each particle is obtained by interpolating the neutral density $n_n(x, y, z)$ to the particle position, similar as the field interpolation in a PIC code. At each time step, for each particle, the accumulated collision probability in the time step is calculated, and a random number P_{ran} evenly distributed between O and 1 is then choscu to determine whether a collision has occured. If a neutral background is present, we may further distinguish whether the ion collide with the plume neutrals or the background neutrals by drawing a second random number P_{ran2}. If a collision has occured to a particle, we obtain the after-collision velocity of the particle! from the equations for conservation of mass, momentum, aud energy.

For electromagnetic simulations, the electromagnetic field is updated from

$$\frac{\partial \vec{E}}{\partial t} = c\nabla \times \vec{B} - \vec{J}, \quad \frac{\partial \vec{B}}{\partial t} = -c\nabla \times \vec{E} \qquad (6)$$

using a charge-consmvation finite-difference leapfrogging scheme[1 8]. The algorithms for 3-D electromagnetic PIC and PIC-MCC simulation were discussed in detail in [14, 15]. For electrostatic simulations, the self-consistent electric field is obtained from the Poisson's equation

$$\nabla^2\Phi = -4\pi\rho \qquad (7)$$

In the code, the Poisson's equation is solved using SOR.

This model is computationally more expensive than the onc developed by Samanta Roy et al[12, 4, 13]. However, this approach allows us to study a wide range of interactions induced by plasma thrusters. For instance, the "intermediate" downstream region and the near-field of a plasma bridge neutralizer where electrons emitted from the neutralizer mix with the ion beam. In this region, electron dynamics plays an important role. Another problem is multiple ion thruster plumes. When multiple ion thrusters are used, primary ion beams from different thrusters may overlap each other. The resulting density profile for the primary ion beam and the production rate of charge-exchange ions are difficult to model correctly in an analytical way, and interactions between two ion beams may be important. These issues may be resolved only through particle simulations for the beam ions. This approach also allows the study of possible beam plasma interactions and the resulting plasma waves and instabilities. This is important for modeling electromagnetic interference problems.

3. Simulations

In this section, we present some preliminary simulation results. Calculations are done using the electrostatic PIC-MCC code on a Cray C90.

The simulation setup is shown in Fig. 1. Due to computational limitations, we are not yet able to perform full scale simulations. Hence, we shall consider a scaled down thruster. The characteristic length scales near an ion thruster exit are the sheath thickness and the thruster radius. Since the ratio of the sheath thickness to Debye length scales as $|e\Phi_T/KT_e|^{3/4}$, we define a quantity ζ

$$\zeta = \frac{|\hat{\Phi}_T|^{3/4}}{\hat{r}_T} \qquad (8)$$

where Φ_T is normalized by electron temperature and $\hat{r}_T$ is normalized by λ_D, where λ_D is the Debye length calculated using the plume density and the initial temperature of the emitting electrons. In our simulations, we choose r_T and Φ_T such that the resulting ζ is the same as that of a real scale thruster. For instance, for a typical 15 cm ion thruster ($r_T \simeq 750\lambda_D$) with a thruster exit potential $\Phi_T \simeq$ 800 Volt, $\zeta \simeq$ 0.2. As in all full particle simulation, computational limitations also require the use of an artificial mass for the ions. In the simulation, we use the artificial ion mass ratio of m_i/m_e = 100.

We take the thruster radius Lo be $r_T = 50\lambda_D$ and $\hat{\Phi}_T$ = −22. This gives a $\zeta \simeq$ 0.2. The neutralizer is modeled by a point source with a volume of 1 cell and potential of $\hat{\Phi}_E$ = --0.2 (Φ_E/Φ_T is in the same range of that in a real scale thruster). The neutralizer is located above the thruster exit (in the y direction). Initially, the simulation domain is a vacuum. At t = 0, we start to inject beam ions from the thruster and electrons from the neutralizer. For simplicity we shall only consider charge exchange collisions here. For a plasma bridge neutralizer, electrons ionize the neutrals surrounding the neutralizer, aud thus creat a plasma bridge. This electron

ionization collision will be included in our future simulations.

The simulation results are shown from Fig. 2 through Fig. 6. In the following, all contour plots are for a xy cutting plane with $z = z_{thruster}$. Hereafter, this plane will be referred to as the "center xy plane". All particle plots are for particles located within a layer of ± 1 cell of the center xy plane. Hereafter, this layer will be referred to as the "center layer".

The neutral plume density contour on the center xy plane is shown in Fig. 2. The initial potential distribution is shown in Fig. 3a. The potential structure is dominated by that due to the surface potential of the thruster, and a uniform sheath covers both the thruster exit and the neutralizer. The neutralizer only causes a small disturbance. In Fig. 3b, we show the positions of the ions and electrons within the center layer after they are injected for the first time.

The beam ions at the end of the simulation is shown in Fig. 4a. Due to their high kinetic energy, The motion of the beam ions are not influenced by the potential field. Collisions between the beam ions and the neutral background generate charge exchange ions. The charge exchange ion production rate is proportional to the neutral density shown in Fig. 2. Fig. 4b shows the positions of the charge exchange ions. In contrast to the beam ions, the motion of the charge exchange ions are greatly influenced by the potential field due to their low kinetic energy.

Fig. 5 shows the potential contours at the end of the simulation. It is interesting to observe that an asymmetric potential distribution has developed. Due to the local ion density enhancement form the beam ion emission, a positive potential "bump" is developed within 1 thruster radius downstream. The potential distributions along the center x axes of the thruster and the neutralizer are plotted on Fig. 5b. We find, along the center x axis of the thruster, the potential peak is about $\Phi_{max} \simeq 12.5$. The potential distribution shown in Fig. 5b is qualitativly in agreement with experimentally measured results. Electrons emitted from the neutralizer are attracted into the plume by this local potential bump. Eventually, the plume becomes quasineutral. (The mixing of electrons with the ion beam is evident in the accompany animation of the simulation results.)

In Fig. 6 we show the phase plot of the charge exchange ions. The potential field influences the charge exchange ions in two ways. First, as shown in Fig. 6a, charge exchange ions produced near the thruster exit will be accelerated towards the thruster exit because they have insufficient kinetic energy to escape the potential well. This backflow may cause potential erosions on the acceleration grids[6, 9] Second, as shown in Fig. 6b, since the plume center has a higher potential, charge exchange ions produced within the plume can flow radially outward the plume region. it is well recognized that, once outside the plume, charge exchange ions may become a potential contamination source.

4. Summary and Conclusions

In support of the NASA SEP Technology Application Program, we are developing 3-D particle simulation models to study a wide range of issues related to ion propulsion. This paper discusses our ongoing study of modeling ion thruster plumes. Preliminary results using, a 3-D (electrostatic full particle, particle-in-cell codes with Monte Carlo collision code are presented for a scaled-down) thruster model. The results are in qualitative agreement with experimental observations. This modeling study is conducted in coordination with ongoing experimental work. Future studies will include model validation using experimental results.

3-D particle simulations of ion thrusters are extremely computational intensive. Currently, we are also developing parallel 3-D PIC and PIC-MCC codes[15, 16]. As Ref[16] shows, we have achieved particle push time/particle/step in the 100 nsecs range and collision time/collision in the 300 nsecs range on a 512-processor Paragon and a 256-processor Cray T3D. Parallel computing techniques and MIMD parallel computers such as the Paragon and T3D will also be utilized in our future studies

Acknowledgement

We would like to thank D. Brinza (JPL), R. Samanta Roy (MIT), and R. Biasca (Northeastern) for many useful discussions. This work was carried out by the Jet Propulsion Laboratory under a contracts from NASA. Access to the Cray C90 was provided by funding from NASA Offices of Mission to Planet Earth, Aeronautics, and Space Science.

References

[1] M.R. Carruth Eds Experimental and analytical evaluation of ion thruster/spacecraft interactions. JPL Publication 80 92, 1981.

[2] M.R. Carruth A review of studies on ion thruster beam and charge-exchange plasmas *AIAA 82-1994*, 1982.

[3] W.D. Deininger Electric propulsion produced environments and possible interactions with the SI'-1OO power system. *AIAA 85-2046*, 1985.

[4] N. Gatsonis, R. Samanta Roy, and D. bastings, Numerical investigation of ion thruster plume backflow, *AIAA 94-3140*,1994.

[5] S. Karmesin, P. Liewer, and J. Wang, 3-D electromagnetic parallel PIC in nonorthogonal meshes, IEEE ICOP'S'95, 1995.

[6] J. Monheiser and P. Wilbur, A n experimental study of impingement ion production mechanisms, *AIAA 92-382 6*,1992.

[7] X. Peng, *W*. Ruyth, and D. Keefer, 3D particle simulation of grid erosion in ion thrusters, *A IA A 91-119,1991.*

[8] X. Peng, W. Ruyth, and D. Keefer, Comparison of 2D and 3D models of grid erosion in an ion thruster, *AIAA 91-2120,1991.*

[9] X. Peng, W. Ruyth, and D. Keefer, Further study of effect of the downstream plasma condition on accelerator grid erosion in an ion thruster, *AIA.1 92-3829,1992.*

[10] J. Polk, J. Brophy, and J. Wang, Spatial and temporal variation of sputter erosion on the accelerator electrode of a 2-Grid, 30-cm ion optics *AIAA 95-2924*, 31st Joint Propulsion Conference, 1995.

[11] R.S. Robinson, H.R. Kaufman, and D.R. Winder Simulation of charge exchange plasma propagation near an ion thruster propelled spacecraft *AIAA 81-0774, 1981.*

[12] R. Samanta Roy, D. bastings, and N. Gatsonis, Modeling of ion thruster plume contamination, *AIAA 95-3138,1994.*

[13] R. Samanta Roy, Numerical simulation of ion thruster plume backflow for spacecraft contamination assessment, Ph.D. thesis, MIT, 1995.

[14] J. Wang, I'. Liewer, and V. Decyk, 3D electromagnetic plasma particle simulations on a MIMD parallel computer, to be published in *Computer Physics Communications*, 1994

[15] J. Wang, R. Biasca, and I'. Liewer, , 3D electromagnetic Monte Carlo particlr+il]-cell simulations of critical ionization velocity experiments in space to be published in *J. Geophys Res.* ,1994

[16] J. Wang, 1'. Liewer, and E. Huang, 3D electromagnetic Monte Carlo particle-in-cell simulations on MIMD parallel computer, *AIAA 95-0593,1995.*

[17] J. Wang, P. Liewer, and S. Karmesin, 3-D PIC using deformable grid for parallel computers Numerical Tokamak Symposium,1995.

[18] J. Villasenor and O. Buneman, Rigorous charge conservation for local electromagnetic field solvers *Computer Phys Comm.*, 69, 1992, pp306-316.

Figure Captions

Figure 1: Model setup

Figure 2: Neutral background density contours on the center xy plane.

Figure 3: Initial conditions, a) initial potential contours on the center xy plane. b) initial beam ion and electron positions.

Figure 4: Beam ion and charge exchange ion positions at end of simulation

F'i.gore 5: Potential field at end of simulation. a) potential contours. b) potential along center axes of the thruster and neutralizer

Figure 6: Phase plot of the charge exchange ions.

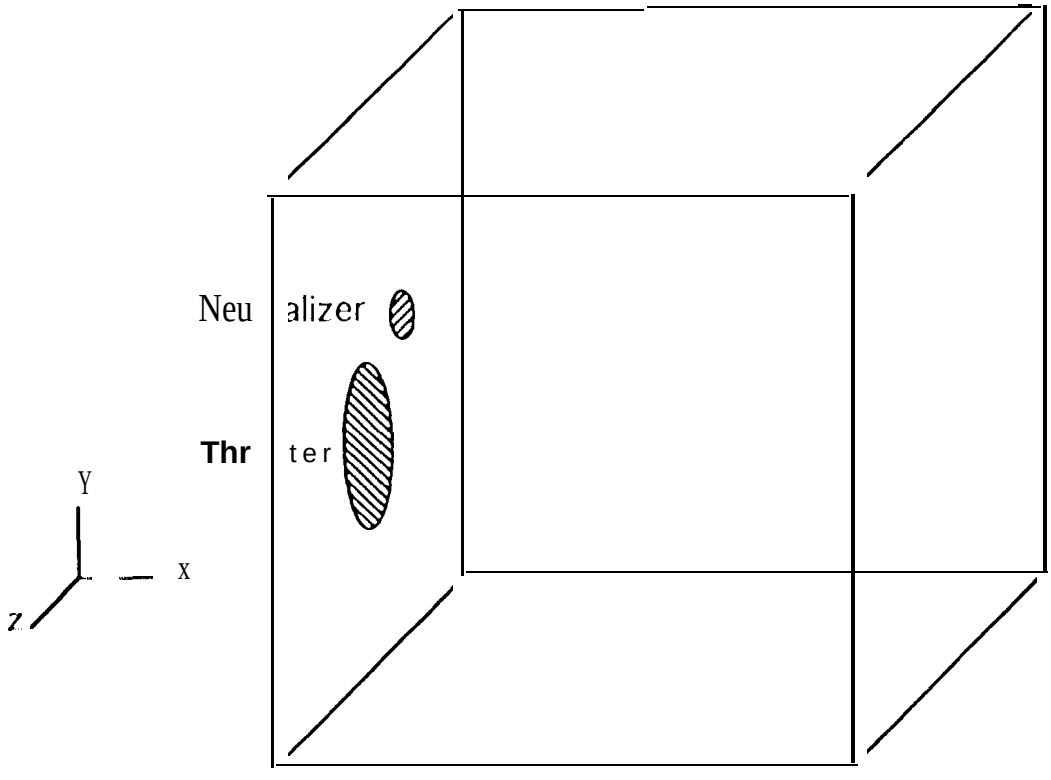

Figure 1

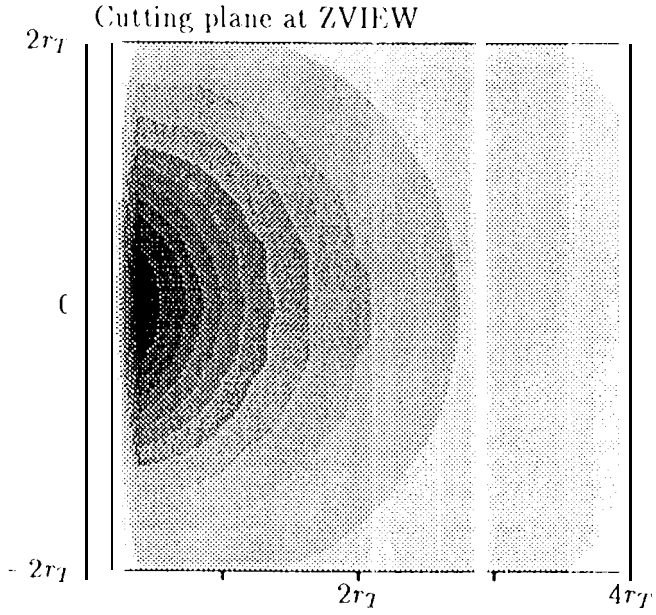

Figure 2

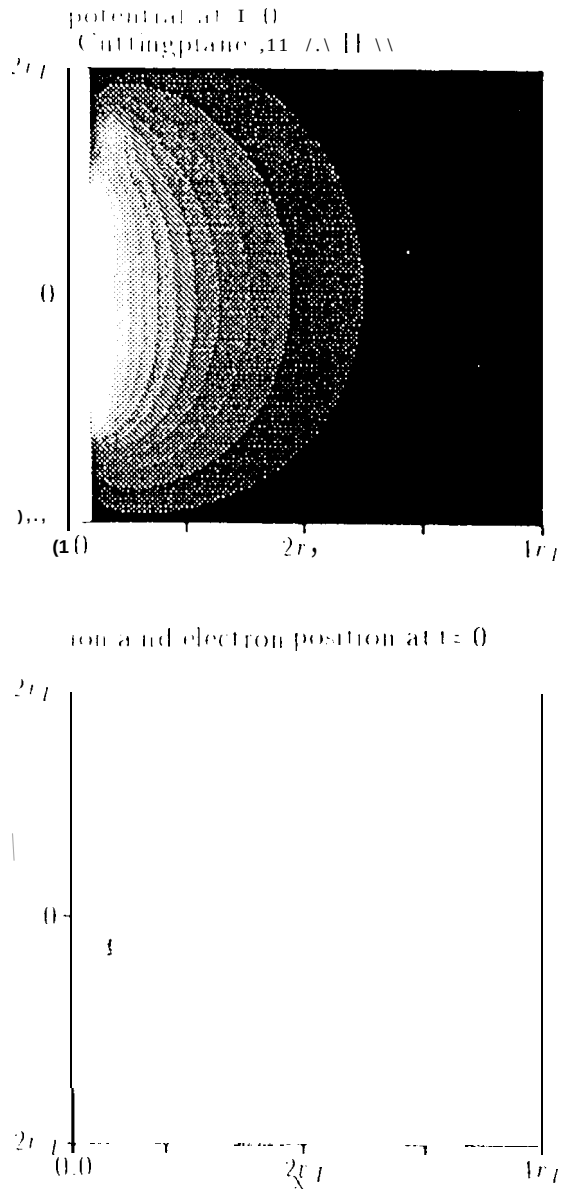

ion and electron position at t = 0

Figure 3

a) beam ion posi ion

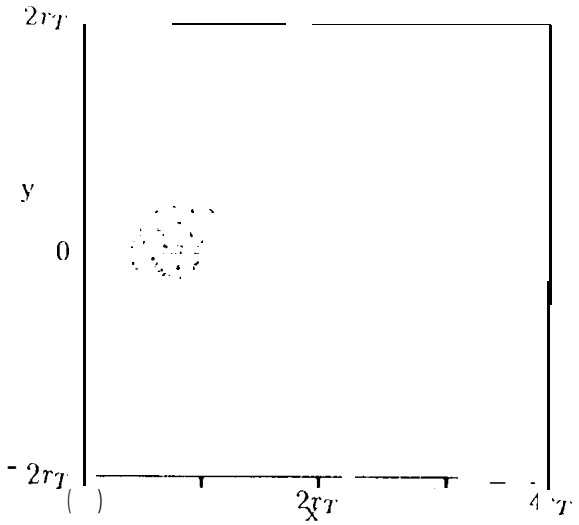

b) cha ge exchange ion position

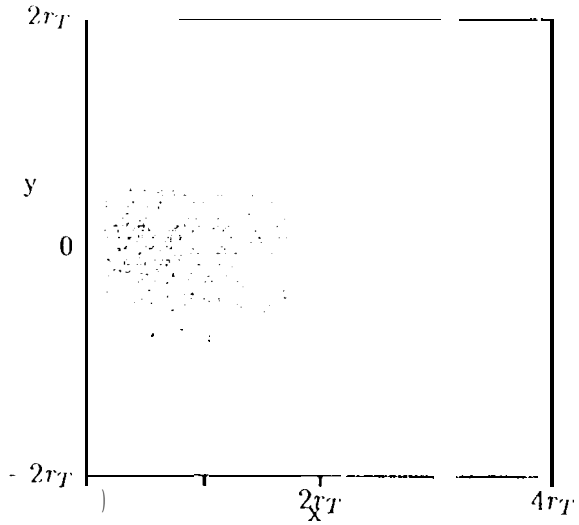

Figure 4

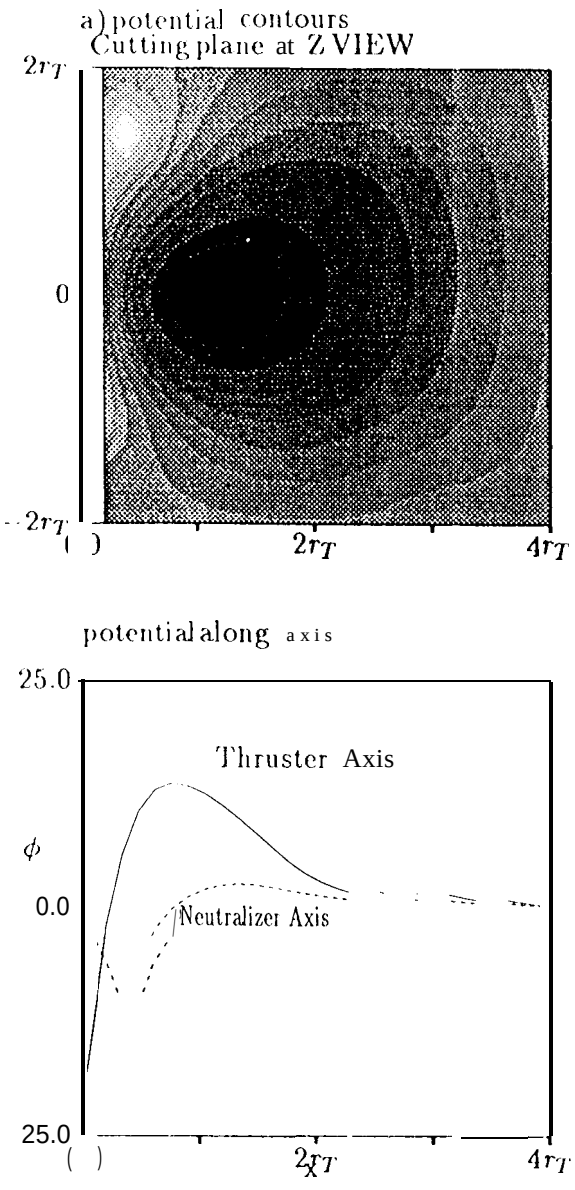
a) potential contours
Cutting plane at Z VIEW
$2r_T$
0
$-2r_T$
( )
$2r_T$
$4r_T$
potential along axis
25.0
Thruster Axis
ϕ
0.0
Neutralizer Axis
25.0
( )
$2r_T$
$4r_T$

Figure 5

a) phase space: v_x vs. x

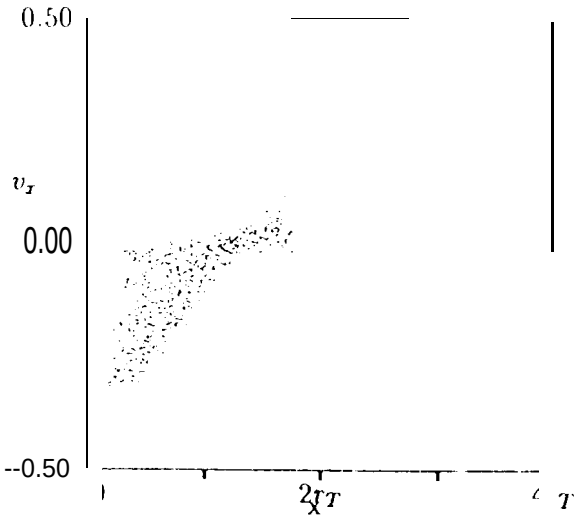

b) phase space: v_y vs. x

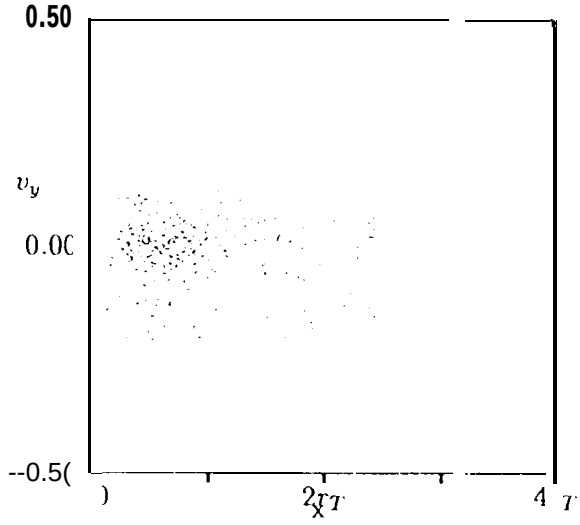

Figure 6